Available online at www.sciencedirect.com
SCIENCE DIRECT®
Mathematics and Computers in Simulation 68 (2005) 201–219
MATHEMATICS AND COMPUTERS IN SIMULATION
www.elsevier.com/locate/matcom

Some global bifurcations related to the appearance of closed invariant curves

Anna Agliari[a,*], Laura Gardini[b], Tönu Puu[c]

[a] *Catholic University, Dipartimento di Scienze Economiche e Sociali, Via Emilia Parmense 84, 29100 Piacenza, Italy*
[b] *Dept. Scienze Economiche, University of Urbino, Urbino 61029, Italy*
[c] *Dept. Economics, University of Umeå, Umeå 90187, Sweden*

Received 13 December 2004; accepted 16 December 2004
Available online 22 January 2005

Abstract

In this paper, we consider a two-dimensional map (a duopoly game) in which the fixed point is destabilized via a subcritical Neimark–Hopf (N–H) bifurcation. Our aim is to investigate, via numerical examples, some global bifurcations associated with the appearance of repelling closed invariant curves involved in the Neimark–Hopf bifurcations. We shall see that the mechanism is not unique, and that it may be related to homoclinic connections of a saddle cycle, that is to a closed invariant curve formed by the merging of a branch of the stable set of the saddle with a branch of the unstable set of the same saddle. This will be shown by analyzing the bifurcations arising inside a periodicity tongue, i.e., a region of the parameter space in which an attracting cycle exists.

Keywords: Discrete dynamical systems; Duopoly models; Subcritical Neimark–Hopf bifurcation; Homoclinic connection

1. Introduction

Economics distinguishes between a number of market forms on the basis of the number of competing firms. Ranging from one supplier, the monopolist, the path goes over two suppliers, duopoly, a few

* Corresponding author. Tel.: +39 0523 599 329; fax: +39 0523 599 303.
E-mail addresses: anna.agliari@unicatt.it (A. Agliari); gardini@econ.uniurb.it (L. Gardini); tonu.puu@econ.umu.se (T. Puu).

0378-4754/$30.00
doi:10.1016/j.matcom.2004.12.003

suppliers, oligopoly, many suppliers, polypoly, to perfect competition. In the last case, each supplier is so small that it cannot in any way influence market price. In the opposite case, the monopolist deliberately limits supply so as to be able to charge a high market price to the end of obtaining a maximum monopoly profit. The cases of duopoly and oligopoly are the most complicated, because each competitor has to take account not only of consumer demand, as reflected in the demand function, but also of the expected retaliations of the competitors. Oligopoly theory is one of the oldest branches of mathematical economics, created in 1838 by the mathematician Augustin Cournot [9].

In Cournot's version, the competitors use their supply as the instrument for competition, and price results from the joint action of the different suppliers. This was, later, harshly criticised by Bertrand [5] in 1883, through a rather confused argument, later made precise by Egdeworth [10]. The argument was that price rather than quantity should be taken as the strategic instrument of the competitors. From this, the theory of product differentiation was born and got its final shape in Chamberlin's famous work [8] of 1932. On the basis of this, economists distinguish between Cournot oligopoly and Bertrand oligopoly. In the long run, however, Cournot's version was not notably affected by the objections, and more has been written about the Cournot version than about any alternative.

Also, very early, it was realized that the Cournot duopoly model might lead to complex dynamics. In 1978, Rand [20] suggested that, under convenient assumptions, duopoly theory would lead to complex dynamic phenomena: orbits of any periodicity, as well as quasi-periodic and chaotic ones, along with multistability, and in the same year Poston and Stewart elaborated this further [19]. In neither, however, any substantial assumptions in terms of economic theory were given for how the shape of the so called reaction functions, i.e., the functions showing how the supply of each dupopolist depended on that of the competitor, might arise. In economics textbooks, these reaction functions were always displayed as straight lines, but Rand suggested upside down parabola shapes, which might even intersect in several points (so called Cournot equilibria).

Such shapes can be obtained in several ways, for instance, through production externalities. The present paper is not a proper place to discuss such diversity and multiplicity. Among the numerous references listed in [21,18], the reader can find many cases where Rand types of reaction functions arise. We just cite the works by Bischi and Kopel [6,7], which emphasize the importance of global analysis in cases with multiple Cournot equilibrium points (also called Nash equilibria in honour of a much later Nobel Prize winning generaliziation of the concept to a game theoretic setting).

The perhaps simplest case, where these Rand type reaction functions arise, was suggested by one of the present authors in 1991. See [16], where the assumption of an isoelastic demand function was just combined with constant marginal costs, and actually resulted in complex dynamics of the types described by Rand and Poston and Stewart.

In its original form, the model has a unique Cournot equilibrium point, and it displays a period doubling cascade to chaos. The same behavior was observed in a modified version, studied in [4], where the regions of positive trajectories of the model were focused, along with the global bifurcations in the attraction basin of the fixed point.

A different dynamic behavior was observed in the "triopoly" case (i.e., assuming three producers instead of two): in [2], it is shown that the Cournot equilibrium point loses stability via a subcritical Neimark–Hopf (N–H) bifurcation, where the repelling invariant curve Γ_u seems to appear with an attracting one (very close to Γ_u), hence resulting in multistability (i.e., the coexistence of two different attractors).

Moreover, the same bifurcation, leading to two closed invariant curves (one attracting and one repelling), was observed in the duopoly models introduced in [16], provided the competitors react through an adaptive

adjustment process, i.e., always move to a weighted average of their previous moves and their calculated new best replies. This is shown, for instance in [15] (though assuming slightly different cost functions) and in [3]. In both these papers, a constraint on the positivity of the quantities produced is explicitly stated. In [3], the appearance of the two invariant curves was related to a particular kind of bifurcations, typical of piecewise smooth maps, the family to which these cases belong. However, the mechanism described there, as an explanation to how the invariant curves are born, is not observed in the entire parameter range. The two invariant curves can also appear far from the constraint, in a way similar to the triopoly case. To our knowledge, this last bifurcation mechanism has not yet been investigated in detail, and this will be the subject of our paper.

Numerical simulations of the maps studied in the works cited above may suggest a saddle–node bifurcation of closed invariant curves, given by the merging of two curves, one attracting and one repelling, followed by their appearance/disappearance (depending on the changes in the parameters). However, as remarked in [13], while this bifurcation is quite common in flows, it is an exceptional case when dealing with two-dimensional maps: In discrete dynamical systems, many global bifurcations involving closed invariant curves are still open problems.

The aim of this paper is to investigate the mechanism involved in the appearance of the two closed invariant curves, in a simpler model than those cited above: Introducing the same economic assumptions as the duopoly model in [16] and an adaptive adjustment process.

We shall see that the bifurcation mechanism may be associated with a pair of cycles, a saddle cycle and an attracting one (node or focus), and the appearance/disappearance may be related to a saddle-connection, called *homoclinic connection*. A homoclinic connection of a saddle is a closed invariant curve formed by the merging of a branch of the stable set[1] of a saddle cycle with a branch of the unstable set of the same saddle, thus forming a closed connection among the periodic points of a saddle cycle. This structurally unstable situation causes a bifurcation between two qualitatively different dynamic behaviors: On one side of the transition closed invariant curves do not exist, while they exist on the other side, and may be homeomorphic to a circle (saddle–node connection or quasiperiodic trajectories) or not (saddle-focus connection). The study of this bifurcation mechanism involves the analysis of the stable and unstable manifolds of the saddle. We check the bifurcation looking at the different dynamic behaviors of the branches. As such a behavior cannot be predicted by a local analysis, the contact between branches strongly depends on the nonlinearity of the map, that is, this bifurcation can be classified as a *global bifurcation*.

The plan of the work is as follows. In the next section, we deduce the duopoly model, its fixed points and their local stability analysis, proving that the Cournot point, say E^*, loses stability via a subcritical N–H bifurcation. In Section 3, we emphasize the bistability regime occurring below the N–H bifurcation curve in the parameter plane, together with the appearance, in the phase plane, of two closed invariant curves. A repelling one, which bounds the basin of attraction of the Cournot point E^* (and is involved in its subcritical N–H bifurcation), and an attracting one, which may be a saddle–node connection or a saddle–focus connection. A periodicity tongue is numerically investigated, and we show that the global bifurcations leading to the closed invariant curves may be homoclinic connections of saddles. Section 3.1 deals with a first homoclinic connection leading to a repelling closed curve and to an attracting saddle–

[1] We recall that the stable and unstable sets of a saddle p^* of a map G are, respectively, defined as

$$W^{\mathrm{S}}(p^*) = \{x : \lim_{n\to+\infty} G^n(x) = p^*\}; \qquad W^{\mathrm{U}}(p^*) = \{x : \lim_{n\to+\infty} G^{-n}(x) = p^*\}.$$

focus connection. Section 3.2 shows a second homoclinic connection leading to another attracting closed invariant curve and to the coexistence of three attractors. Section 3.3 illustrates a conjecture, associated with a generic bifurcation leading (always via a homoclinic connection) to the appearance of the two closed invariant curves as saddle–node connections. Section 4 concludes.

2. The model

The model we consider is the two-dimensional map

$$M : \begin{cases} x' = x + \lambda \left(\sqrt{\dfrac{y}{k}} - x - y \right) \\ y' = y + \lambda \left(\sqrt{x} - x - y \right) \end{cases} \tag{1}$$

where the symbol prime ($'$) denotes the unit time advancement operator, i.e., if x is the value at time, $t-1$, x' denotes the value at time t.

The map M in (1) depends on two parameters (λ, k) and, as we shall see in the next subsection, economic considerations lead us to consider $\lambda \in (0, 1)$ and $k > 1$. Hence, the region of interest in the parameter plane is

$$\Omega = (0, 1) \times (1, \infty).$$

The map M is defined only in the positive quadrant of the plane $\mathbb{R}^+$ (where we include the axes, that is, $x \geq 0$ and $y \geq 0$), which is not a trapping set. Thus, a first problem arises in studying M, related to the determination of the set, say F, in which the orbits of the dynamic model are well defined, i.e., the set

$$F = \{(x, y) \in \mathbb{R}^+ : M^n(x, y) \in \mathbb{R}^+ \ \ \forall n \geq 0\}. \tag{2}$$

We analyzed a similar problem in [3], where it was shown that the region F is bounded by the preimages[2] of the y-axis, obtained in a finite number of steps, or as a limit set of the preimages. In particular, the rank-1 primage of the vertical axis is a curve issuing from the point $(0, 1/k)$ of the phase plane. Thus, increasing the value of the parameter k, the region F in which the map is a dynamical system decreases in size. And at high values of k, for the map M in (1), the boundary of the set F plays an important role in the appearance of a single repelling closed invariant curve Γ_u. In fact, when the number of preimages giving F tends to infinity then Γ_u appears: it is the boundary of the region F and also the boundary of the basin of the stable fixed point. However, in this paper, we are interested in lower values of k, for which the region F is quite wide, and its shape is not relevant to our study. Our object is to investigate the appearance (inside F) of the repelling closed invariant curve Γ_u which, at low values of k, is often related to the appearance of also an attracting one, Γ_a, as shown in Fig. 1a. Γ_u always bounds the basin of attraction of E^*. Fig. 1b and c will be discussed in Section 3.

As stated in the introduction, the aim of the present paper is to study some global bifurcations related to the appearance of two such curves. Before this, let us give a short explanation of the economic context in which the map (1) has its foundation, and perform the local stability analysis of its fixed points, preliminary to our study.

[2] Observe that the map M is noninvertible. However, the bifurcations described in this paper do not involve this property of the map. For this reason, we do not present here the related Riemann foliation of the phase plane, which can be found in [3].

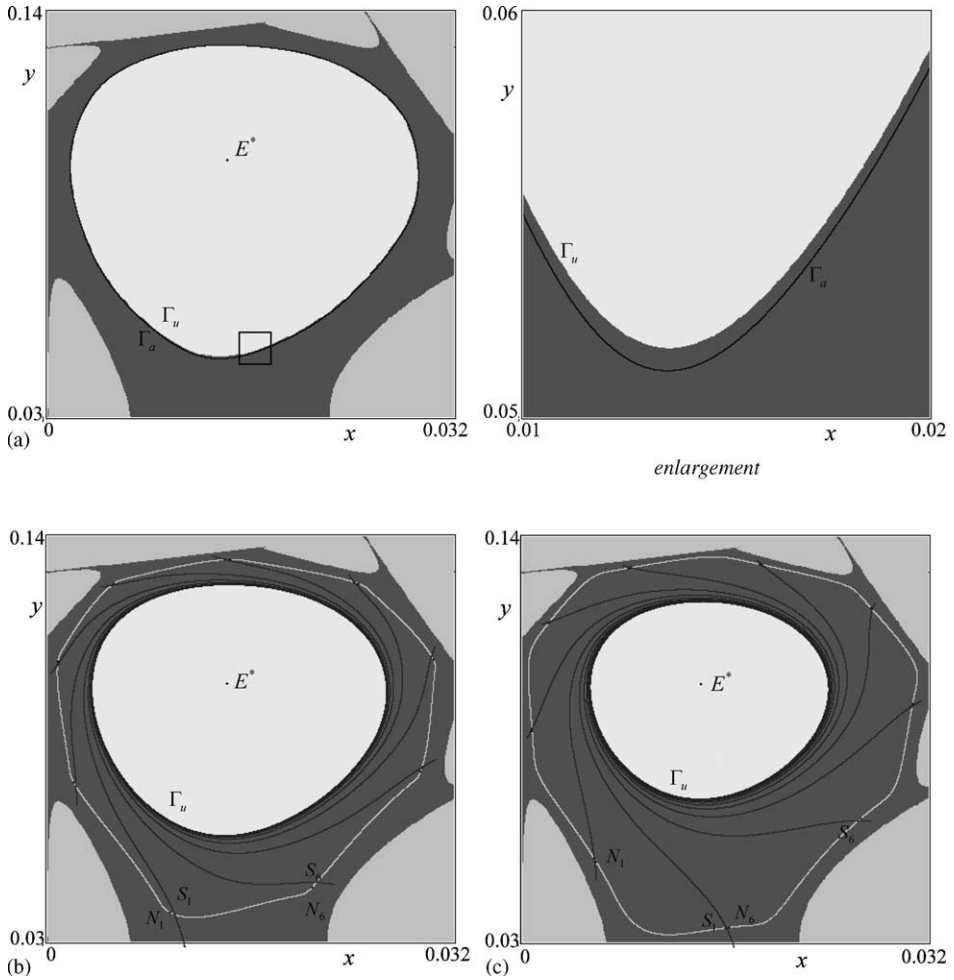

Fig. 1. (a) $k = 7.40007; \lambda = 0.835$. Appearance of the repelling closed invariant curve Γ_u related also to the appearance of an attracting one, Γ_a. The enlargement corresponds to the square in (a). (b) $k = 7.40715; \lambda = 0.835$. The attracting curve Γ_a consists in the saddle-node connection. (c) $k = 7.419; \lambda = 0.835$. The periodic point S_1, born together with N_1, moves towards N_6.

2.1. The economic model

The map M in (1) comes from an economic application, that we shall briefly illustrate (for a more exhaustive introduction see [3,16,17]). It describes the strategic behavior of two competitors which produce an homogeneous good. In this contest, Cournot's duopoly theory suggests that each competitor has to produce the quantity maximizing its profit, which depends on the expected production of the opponent.

We assume that

- the demand function of the good is isoelastic, i.e., $Q = 1/p$, where Q is the total demand and p is the price of the good;

- the costs are linear, $C_i(q) = c_i q$, where the marginal costs c_i are positive.

From these hypotheses, one immediatly obtains the profit function:

$$U_i(q_i, q_j) = \frac{q_i}{q_i + q_j} - c_i q_i, \tag{3}$$

where $i, j = 1, 2$, $j \neq i$ and $q_i \geq 0$ are the quantities of the two producers.

The optimal choice of competitor i, given the expected production of its opponent, q_j^{e}, is

$$R_i(q_j^{\mathrm{e}}) = \sqrt{\frac{q_j^{\mathrm{e}}}{c_i}} - q_j^{\mathrm{e}}. \tag{4}$$

This is usually called the *best reply function*, or *reaction function*.

If the two firms have full information about the market and the competitor, they immediately choose the intersection point of the two reaction functions, that is, the so called *Cournot equilibrium point*

$$E^* = (q_1^*, q_2^*) = \left(\frac{c_1}{(c_1 + c_2)^2}, \frac{c_2}{(c_1 + c_2)^2} \right) \tag{5}$$

Here, we assume that the two firms at each stage expect production of the competitor to remain the same as in the previous period, i.e.,

$$q_i^{\mathrm{e}}(t) = q_i(t - 1). \tag{6}$$

Moreover, at each step, knowing their lack of information about the move of the opponent, the competitors do not immediately jump to the optimum predicted by the best reply function. So, they adaptively adjust their previous decision in the direction of the new optimum:

$$\begin{cases} q_1(t) = (1 - \lambda) q_1(t - 1) + \lambda R_1(q_2(t - 1)) \\ q_2(t) = (1 - \mu) q_2(t - 1) + \mu R_2(q_1(t - 1)) \end{cases} \tag{7}$$

where λ and μ are the two adjustment speeds ($0 < \lambda, \mu < 1$).

Substituting in (7) the best reply functions (4), and using the assumption in (6), we obtain the following two-dimensional map

$$T : \begin{cases} x' = (1 - \lambda) x + \lambda \left(\sqrt{\dfrac{y}{c_1}} - y \right) \\ y' = (1 - \lambda) y + \mu \left(\sqrt{\dfrac{x}{c_2}} - x \right) \end{cases} \tag{8}$$

where the variables x and y denote the quantities q_1 an q_2, respectively.

Finally, the map M we are looking for is topologically conjugated to the map T in (8) with $\lambda = \mu$. In fact, it can be proved (see [3]) that the marginal costs (c_1, c_2) can be replaced (via a change of coordinates) by $(k, 1)$ with $k = c_1/c_2$. Thus, assuming $k > 1$, as we do, we simply mean that the index 1 denotes the producers with higher marginal cost.

2.2. Fixed point and local stability

In this subsection, we study the local stability of the fixed points of the map M in (1), as the parameters (λ, k) vary in the region of interest, that is $\Omega = (0, 1) \times (1, \infty)$.

It is simple to obtain the fixed points, which are

$$O^* = (0, 0)$$
$$E^* = \left(\frac{1}{(k+1)^2}, \frac{k}{(k+1)^2}\right).$$

As usual, we study the local stability of a fixed point by using the eigenvalues of the Jacobian matrix of M, which is given by

$$J(x, y) = \begin{bmatrix} 1-\lambda & \lambda\left(\dfrac{1}{2\sqrt{ky}} - 1\right) \\ \lambda\left(\dfrac{1}{2\sqrt{x}} - 1\right) & 1-\lambda \end{bmatrix}. \tag{9}$$

From (9), we deduce that in O^*, the map is not differentiable, but as (x, y) tends to $(0, 0)$ one eigenvalue of $J(x, y)$ tends to infinity, and O^* results in an unstable fixed point.

For the other fixed point E^*, we can state the following:

Proposition 2.1. *The fixed point E^* is a stable focus in the subset of Ω defined by*

$$\Omega_{\text{stab}} = \{(k, \lambda) : 0 < \lambda < f(k)\} \tag{10}$$

where

$$f(k) = \begin{cases} 1 & \text{if } 1 < k \leq 3 + 2\sqrt{2}, \\ \dfrac{8k}{(1+k)^2} & \text{if } k > 3 + 2\sqrt{2}. \end{cases}.$$

Proof. The Jacobian matrix at the fixed point E^* is

$$J^* = \begin{bmatrix} 1-\lambda & \lambda\dfrac{1-k}{2k} \\ \lambda\dfrac{k-1}{2} & 1-\lambda \end{bmatrix} \tag{11}$$

and its characteristic polynomial can be written as

$$p(S) = [S - 1 + \lambda]^2 + \frac{\lambda^2(1-k)^2}{4k}.$$

Given the positivity of the parameter k, it is immediate to observe that $p(S)$ has always the complex roots

$$S = 1 - \lambda + i\frac{\lambda(k-1)}{2\sqrt{k}} \tag{12}$$

and its conjugate $\overline{S}$, i.e., the fixed point E^* is a focus. Moreover, the eigenvalues are inside the unit circle (and E^* is stable), if and only if

$$|S|^2 = (1-\lambda)^2 + \frac{\lambda^2(1-k)^2}{4k} < 1. \tag{13}$$

Solving (13) with respect to λ and recalling that such a parameter must be less than 1, we obtain as solution set exactly Ω_{stab} described in (10).

The stability region of the fixed point is shown in Fig. 2. The portion of the curve $\lambda = 8k/(1+k)^2$ belonging to the frontier of the set Ω_{stab} defines a *N–H bifurcation curve*, i.e., the locus of parameter values at which a N–H bifurcation takes place.

Proposition 2.2. *If $k > 3 + 2\sqrt{2}$, at the bifurcation values*

$$\lambda = \frac{8k}{(k+1)^2} \tag{14}$$

a subcritical Neimark–Hopf bifurcation takes place.

Proof. From Proposition 2.1, we have that the complex eigenvalues of $J(E^*)$ in (11) have modulus one when (14) holds. Moreover, it is simple to verify that if $\lambda < 1$ and $k > 3 + 2\sqrt{2}$, then $|S|^j \neq 1$, $j = 2, 3, 4$. This proves that crossing the curve in (14) a N–H bifurcation takes place. Finally, computing the coefficients d and a of Theorem 3.5.2 in [11] (p.162), for $\lambda < 1$ and $k > 3 + 2\sqrt{2}$ we obtain $d = 1$ and $a < 0$. This proves that the N–H bifurcation is of subcritical type. □

Now, our aim is to investigate the subcritical N–H bifurcation. From Proposition 2.2, we know that crossing (from below) the bifurcation curve in (14), an invariant repelling closed curve, coexisting with

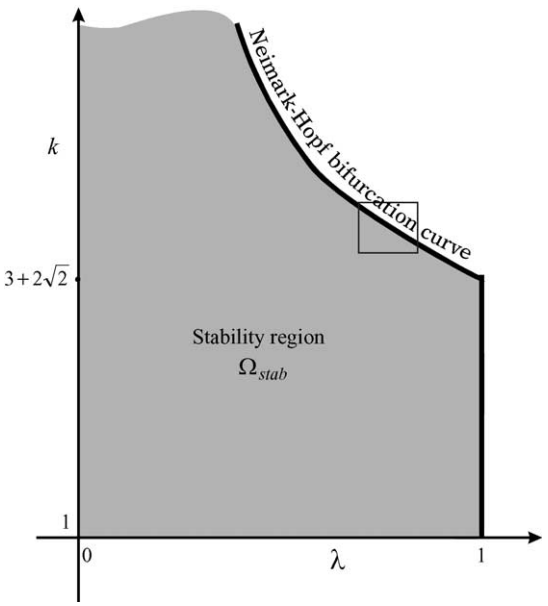

Fig. 2. The stability region of the fixed point E^*. The light gray square denotes the area shown in Fig. 3.

the stable focus E^* and bounding its basin of attraction, must collapse in E^*, which becomes unstable after the bifurcation. The next section is devoted to this invariant repelling closed curve: we shall investigate the global bifurcation leading to its appearance.

3. Appearance of invariant closed curves

As we have proved in the previous section, we are faced with a subcritical N–H bifurcation of the fixed point E^*, so that we cannot expect to find in the (λ, k) parameter plane, above the bifurcation curve, Arnold tongues like those occurring in the supercritical case. However, as the invariant curves appear before the N–H bifurcation, the search of attracting cycles may be a helpful starting point also in our analysis. Looking at the bifurcation diagram for the map M in (1), we can observe some narrow regions in which an attracting cycle exists. They are very few, very thin and with a tongue-like shape. We shall call them periodicity tongues. An example is shown in Fig. 3, in which an enlargement of Fig. 2 shows a periodicity tongue related to a cycle of period 9 (with rotation number 2/9): Such a tongue originates below the Neimark–Hopf bifurcation curve and persists also after the bifurcation.

It is worth to note that the periodicity tongues appear only when the parameter λ is quite large (greater than 0.7). This may be related to the fact that at small values of λ the N–H bifurcation occurs at large values of the parameter k, and when k is large the definition set F in (2) is very small. This case (say $\lambda < 0.7$ and high values of k) is similar to the one considered in [3], and the bifurcation mechanisms leads only to a repelling closed invariant curve. Such a curve results as the limit set of the preimages of the y-axis, and when Γ_u appears it is tangent to the y-axis: It is the frontier of the definition set F and also the boundary of the basin of attraction of the fixed point (merging with it at the bifurcation value). Thus, the appearance of Γ_u is strictly related with the definition set of the map M, and it is impossible to have also an attracting closed curve or a cycle external to Γ_u (as it should belong to the region in which the map is not defined).

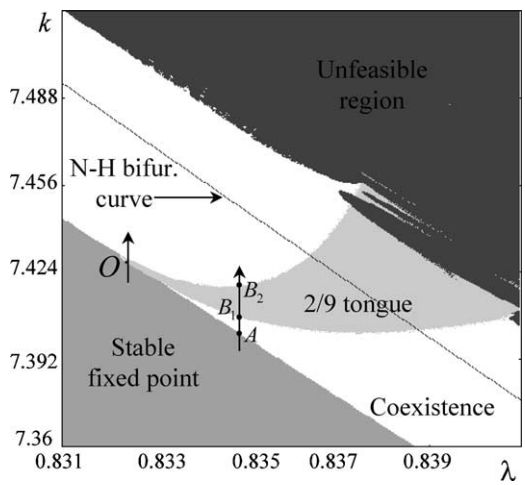

Fig. 3. A periodicity tongue related to a cycle of period 9 (with rotation number 2/9). The points A, B_1, B_2 correspond to the parameter values of Fig. 1. Sequences of parameter values close to the point O have been considered in Sections 3 and 4.

A different situation arises for $\lambda > 0.7$ when the parameter k is small, and the set F is larger: at its first appearance the curve Γ_u is inside F, quite far from the coordinate axes, and also associated with an attracting one (Γ_a). This is the case illustrated in Fig. 1a. The values of the parameters in Fig. 1a correspond to those of the point A in Fig. 3.

Let us explain first the different regions evidenced in this figure. When the parameters (λ, k) belong to the lower gray region of Fig. 3, or to the white strip below the N–H curve, the fixed point E^* is stable. For (λ, k) belonging to the white strip between the gray region and the N–H curve, besides the fixed point, at least one other attractor exists. Inside the $2/9$ periodicity tongue, one of the attractors is a cycle of period 9. The boundary of the gray region denotes the existence of a global bifurcation leading to the appearance of a repelling invariant curve Γ_u. The boundary of the $2/9$ periodicity tongue is generally a saddle-attracting node bifurcation. An example is given in Fig. 1b and c, increasing the value of k from the point A , following the arrow shown in Fig. 3. When the parameters (λ, k) are in the point B_1 of Fig. 3, we enter the $2/9$ periodicity tongue: a saddle–node occurs on the attracting closed invariant curve Γ_a, in Fig. 1b the periodic points of the saddle are very close to those of the attracting node. This bifurcation is the analogue of a p/q frequency-locking in a standard Arnold tongue (cf. [22–24]). Inside a tongue a periodic orbit of period q exists such that the iteration visit all the q periodic points after p turns around the fixed point, and so the tongue is associated with the rotation number p/q ($2/9$ in Fig. 3). As it is shown in Fig. 1b, soon after the bifurcation, the attracting curve Γ_a consists in the saddle–node connection: the unstable branches of the saddle reach the node, constituting Γ_a (while the stable branches of the saddle are transverse to Γ_a). As k increases further, the points of the saddle move: the periodic point S_1 (see Fig. 1b), born together with N_1, moves towards N_6 (see Fig. 1c) and merges with N_6 (in a second saddle–node bifurcation) when the parameters (λ, k) reach B_2, the other boundary point of the $2/9$ periodicity tongue. Increasing k further, outside the $2/9$ periodicity tongue, we still have an attracting invariant closed curve Γ_a, and the numerical simulations show a trajectory on Γ_a which seems quasiperiodic. However, it is worth to note that this may be due to numerical truncation errors, and the true orbit may also be associated with a pair of cycles of high period.

Γ_u always bounds the basin of attraction of the fixed point E^*, and it shrinks to E^* as the parameters approach the N–H bifurcation curve.

As we have seen above, inside a p/q periodicity tongue, generally the invariant attracting curve is given by a *saddle–node connection*. However, the attracting invariant curve may also be given by a *saddle–focus connection* (i.e., the unstable set of the saddle connects the periodic points of the focus). The difference between the two situations is that in the first case the closed curve is homeomorphic to a circle while in the second one, this does not occur, due to the spiraling of the unstable manifold of the saddle around the focus. Indeed a saddle–focus connection has been observed when the parameters (λ, k) are taken close to the origin of the periodicity tongue. We increase k moving the point along the arrow near O in Fig. 3, and the corresponding dynamic behavior is described in the next subsections.

3.1. First homoclinic connection and saddle–focus connection

To explain the mechanism which leads to the two closed invariant curves, let us first investigate a particular situation of the $2/9$ periodicity tongue in Fig. 3, choosing the parameters near the origin (point O in Fig. 3), in order to cross from the gray region directly into the periodicity tongue, avoiding the white strip (which exists above the point A in Fig. 3).

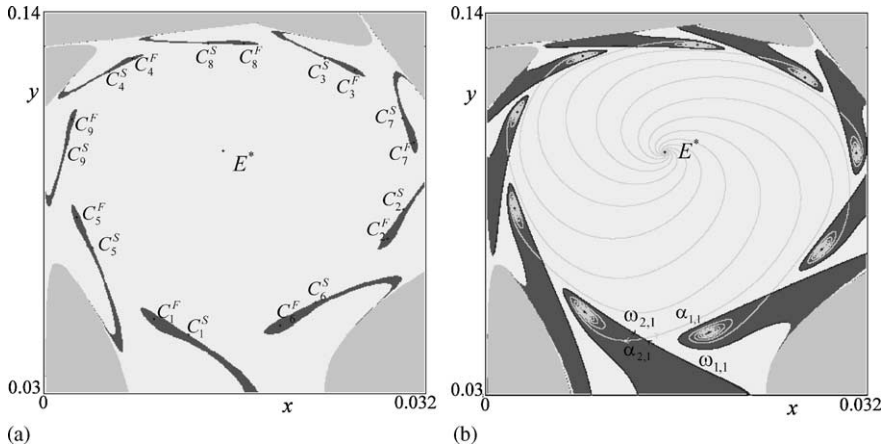

Fig. 4. (a) $k = 7.4278; \lambda = 0.8324$. An attracting focus cycle C^F of period 9 exists together with a saddle cycle C^S of the same period. The fixed point E^* is stable. The stable set of the saddle C^S separates the basins of attraction of C^F and E^*, gray and light gray points, respectively. (b) $k = 7.4285; \lambda = 0.8324$. The basin of attraction of C^F (always bounded by the the stable set of the saddle) is larger. The two branches of the stable set ($W_1^S(C^S) = \cup\omega_{1,i}$ and $W_2^S(C^S) = \cup\omega_{2,i}$), and of the unstable one ($W_1^U(C^S) = \cup\alpha_{1,i}$ and $W_2^U(C^S) = \cup\alpha_{2,i}$), of the saddle are also represented.

In the following analysis, we fix $\lambda = 0.8324$ and increase k, moving the point in the parameter plane along a vertical path inside the 2/9 periodicity tongue, close to O. The starting value is $k = 7.4278$ (see Fig. 4a), and in the phase space an attracting focus cycle C^F of period 9 exists, as well as a saddle cycle C^S of the same period, and the fixed point E^* is still stable. The stable set of the saddle C^S separates the basins of attraction of C^F and E^*, $\mathcal{B}(C^F)$ and $\mathcal{B}(E^*)$, respectively (gray and light gray points in Fig. 4a). The small shape of the basin of C^F suggests that we are quite close to the bifurcation which has given rise to such an attracting cycle.

As the parameter k is increased, the basin of attraction of C^F (always bounded by the stable set of the saddle) becomes larger, as we can see in Fig. 4b, in which also the two branches of the stable set ($W_1^S(C^S) = \cup\omega_{1,i}$ and $W_2^S(C^S) = \cup\omega_{2,i}$), and of the unstable one ($W_1^U(C^S) = \cup\alpha_{1,i}$ and $W_2^U(C^S) = \cup\alpha_{2,i}$), of the saddle are indicated. We observe that the boundary of the basin $\mathcal{B}(C^F)$ is given by $W_1^S \cup W_2^S$ whereas the unstable branch W_1^U converges to E^* and W_2^U tends to the cycle C^F. Observe also that each portion $\omega_{1,i}$ of the stable branch, turning around a periodic point of the focus approaches another periodic point of the saddle. This is more evident in Fig. 5 and its enlargement. In this figure, we can see that $\mathcal{B}(E^*)$ has a "spider" shape with nine thin strips as "legs": this means that the two branches, W_1^S and W_2^S, of the stable set of the saddle are close to each other and, as we can appreciate in the enlargement of Fig. 5, the branch W_1^S is very close to the branch W_1^U. More precisely, we have that the unstable branch $\alpha_{1,i}$ of the saddle periodic point C_i^S is very close to the stable branch $\omega_{1,i+5}$ of C_{i+5}^S. This denotes that we are close to a global bifurcation. In fact, if we slightly increase the parameter k, as in Fig. 6, an invariant closed curve Γ_u bounds the basin of attraction of the fixed point and an attracting closed invariant curve Γ_a exists, given by the saddle–focus connection.

Note that after the bifurcation the unstable branch $\alpha_{1,i}$ has a different asymptotic behavior: it no longer converges to E^* but to the periodic point C_{i+5}^F, whereas the dynamic behavior of $\alpha_{2,i}$ is not changed, it still goes to C_i^F. The stable set of the saddle cycle separates the basin of the nine stable fixed points C_i^F of the map M^9, and Γ_u is the limit set of the branch W_1^S. This proves that the bifurcation giving rise to

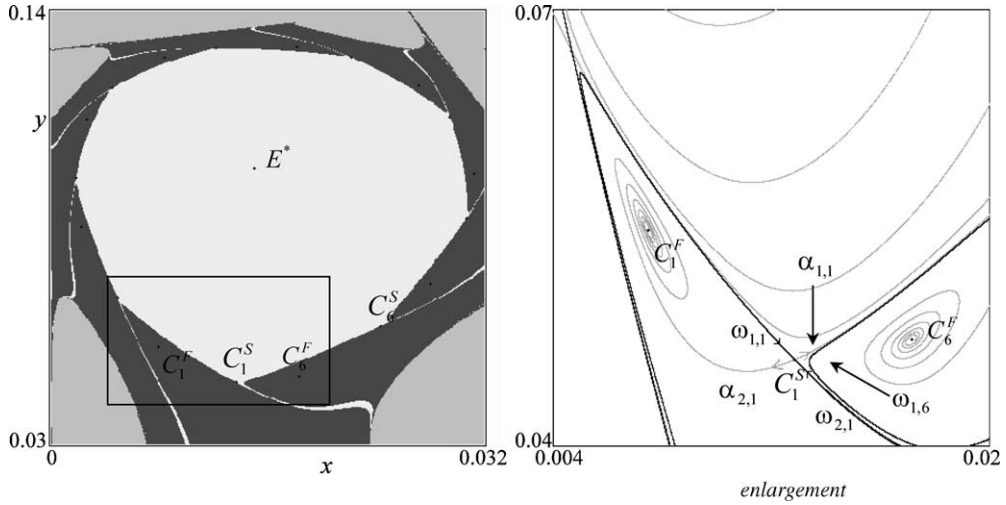

Fig. 5. $k = 7.4288; \lambda = 0.8324$. The basin of attraction of E^* has a "spider" shape with nine thin strips as "legs" : this means that the two branches, W_1^S and W_2^S, of the stable set of the saddle are close to each other. In the enlargement of the rectangular portion the unstable branch $\alpha_{1,1}$ of the saddle periodic point C_1^S is very close to the stable branch $\omega_{1,6}$ of C_6^S.

Γ_u must involve the two branches of the stable and unstable set of the saddle, which have changed their behavior, and we can explain such a change assuming an *homoclinic connection* at the bifurcation value. The homoclinic connection is given by the merging of a branch of the stable set of a periodic point of a saddle cycle, with the unstable branch of another periodic point of the same saddle, forming an invariant closed curve connecting the periodic points of the saddle (for example, in our case, at the bifurcation $\omega_{1,i+5}$ merges with $\alpha_{1,i}$, and so on cyclically). This structurally unstable situation causes the bifurcation

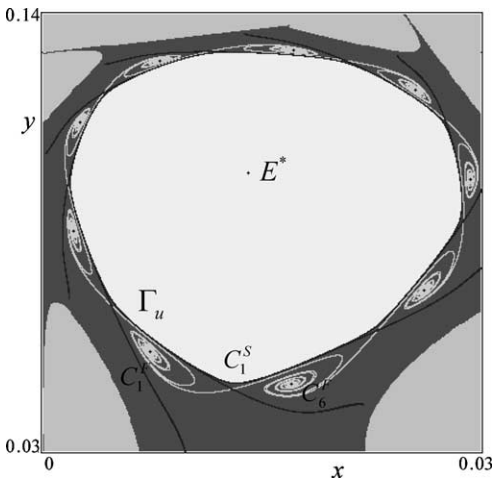

Fig. 6. $k = 7.4289; \lambda = 0.8324$. At a slight increased value of k (with respect to the one used in Fig. 5) an invariant closed curve Γ_u bounds the basin of attraction of the fixed point and an attracting closed invariant curve Γ_a exists, given by the saddle–focus connection. Note the different asymptotic behaviors of the unstable branch W_1^U and of the stable one W_1^S.

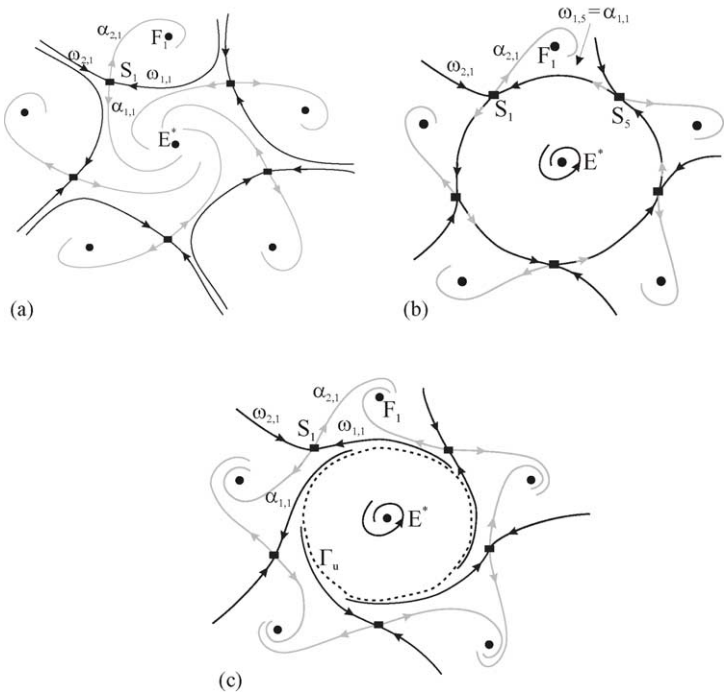

Fig. 7. Qualitative representation of an homoclinic connection which may cause the appearance of a repelling closed invariant curve and a saddle–focus connection.

between the two qualitatively different dynamical behavior we detected (no closed curves on one side, two closed curves on the other side).

We summarize in Fig. 7, a qualitative sketch of this bifurcation (referring to hypothetical cycles of period 5 with rotation number 1/5). Before the bifurcation, Fig. 7a, an attracting focus cycle coexists with the stable fixed point; the basins of attraction of the two attractors are separated by the stable manifold of the saddle cycle. The unstable branch $W_1^{\mathrm{U}} = \cup\alpha_{1,i}$ tends to the fixed point and $W_2^{\mathrm{U}} = \cup\alpha_{2,i}$ to the focus cycle. As the bifurcation value is approached, the stable branch $\omega_{1,i}$ of the saddle periodic point S_i approaches the unstable branch $\alpha_{1,j}$ of S_j, so preparing the homoclinic connection. At the bifurcation (Fig. 7b) we have that the two branches $\omega_{1,i}$ and $\alpha_{1,j}$ merge giving rise to a connection between the periodic points of the saddle cycle: the attracting cycle is external to such a connection and the branch W_2^{U} still converges to it. The stable fixed point is internal to the saddle connection which bounds its basin of attraction. Immediately after the bifurcation, an invariant repelling close curve is created (from which the branch W_1^{S} comes out, rolling up). The unstable branch W_1^{U} converges to the focus cycle, creating with W_2^{U} another closed invariant curve, attracting, given by the saddle–focus connection (see Fig. 7c).

3.2. Second homoclinic connection and three attractors

In the previous subsection, we have seen a mechanism leading to the appearance of the invariant repelling closed curve Γ_u (which will be involved in the subcritical N–H bifurcation), and an attracting

one, made up by a saddle–focus connection. Thus, the parameters used in Fig. 6 belong to the 2/9 periodicity tongue, and the stable cycle is a focus. Increasing k we shall see the disappearance of the cycle of period 9, but this will occur after a second homoclinic connection.

An invariant attractive closed curve Γ_a will be created by a mechanism similar to the one previously described, but now involving the stable branch W_2^S and the unstable one W_2^U of the saddle cycle. Let us start from the situation shown in Fig. 6: here the unstable branch W_2^U converges to the attracting focus and the stable manifold W_2^S comes from the boundary of the set F (defined in (2)) and separates the basins of attraction of the 9 periodic points of C^F. As the parameter k increases, each of the components $\alpha_{2,i+5}$ of W_2^U comes closer and closer to $\omega_{2,i}$, belonging to the stable set W_2^S (see Fig. 8 and its enlargement). A contact between these two branches is then expected. In fact, further increasing the parameter k (i.e., soon after the bifurcation),we observe that the two branches change their dynamical behavior (Fig. 9a). The limit set of W_2^U is now an attracting invariant closed curve Γ_a, created by the *homoclinic connection* occurring at the bifurcation value. W_2^S always separates the basins of the periodic points of C^F for the map M^9, which are drastically reduced in size.

As a consequence, the dynamical system has three coexisting attractors: the fixed point E^* (whose basin of attraction is bounded by the repelling curve Γ_u), the attracting curve Γ_a and the focus-cycle C^F of period 9. Thus, we are still inside the 2/9 periodicity tongue. However, the two cycles of period 9 are no longer connected, as they do not belong to a closed invariant curve. In fact, the basin of attraction of C^F and Γ_a are separated by the stable set of the saddle cycle C^S, which rolls up from Γ_u. The coexistence of the three attractors persists until the "death" of the two cycles, which occurs via a saddle–node bifurcation (i.e., the focus cycle turns into node before merging with the saddle), as usually occurs at the exit of a periodic tongue. This can be observed in Fig. 9b, in which the basin of attraction of C^F is very small, being the parameters close to the saddle–node bifurcation.

A qualitative sketch of the second homoclinic connection is given in Fig. 10, involving cycles of period 5: the starting situation (Fig. 10a) assumes the existence of a heteroclinic connection between a focus-

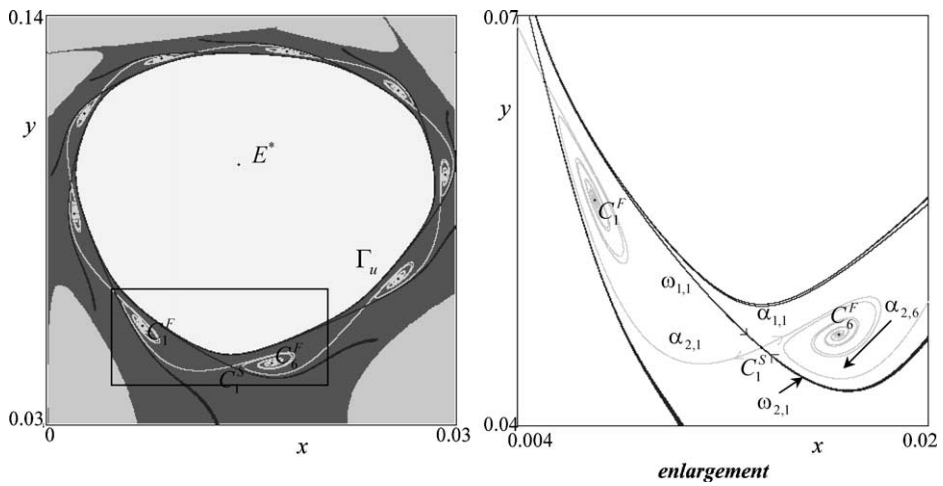

Fig. 8. $k = 7.4292; \lambda = 0.8324$. As the parameter k increases, each of the components $\alpha_{2,i+5}$ of W_2^U comes closer and closer to $\omega_{2,i}$, belonging to the stable set W_2^S ($\alpha_{2,6}$ and $\omega_{2,1}$ in the enlargement).

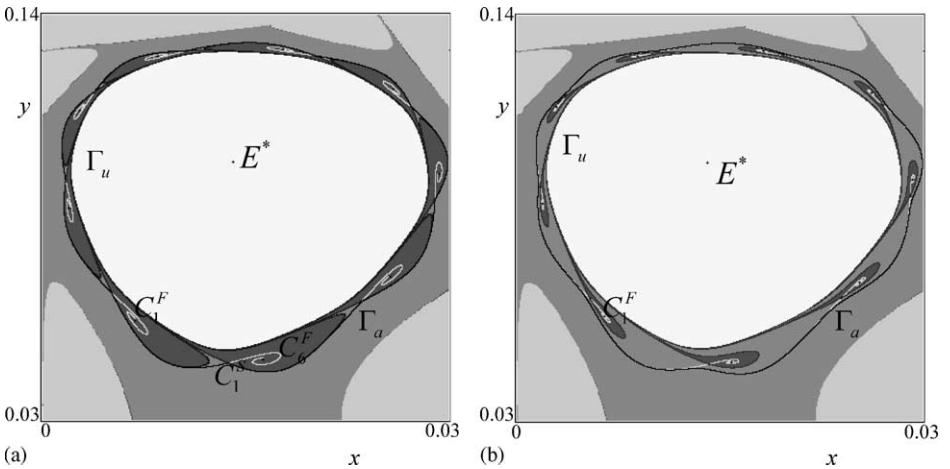

Fig. 9. (a) $k = 7.4293; \lambda = 0.8324$. Coexistence of three attractors. The limit set of W_2^{U} is an attracting invariant closed curve Γ_a, created by the homoclinic connection. The basin of attraction of C^{F} and Γ_a are separated by the stable set of the saddle cycle C^{S}, which rolls up from Γ_u (b) $k = 7.4295; \lambda = 0.8324$. The basin of attraction of C^{F} is very small, being the parameters close to the saddle–node bifurcation.

cycle and a saddle cycle (the unstable manifold of the saddle reaches the periodic points of the focus), a repelling closed curve Γ_u exists, boundary of the basin $\mathcal{B}(E^*)$, limit set of the branch W_1^{S} of the stable set of the saddle. At the bifurcation value (Fig. 10b) the homoclinic connection of the periodic points of the saddle takes place, due to the merging of the unstable branch W_2^{U} with the stable one W_2^{S}. Its effect

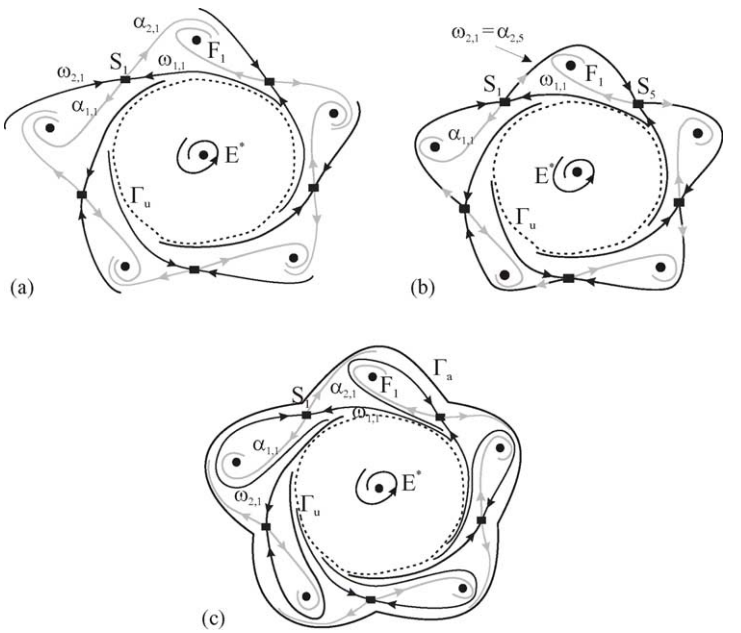

Fig. 10. Qualitative representation of an homoclinic connection which may cause the appearance of an attracting closed invariant curve around a stable focus cycle.

is the creation of an attracting closed curve which encloses the cycle and the repelling curve. After the bifurcation, Fig. 10c, we obtain three different attractors. The homoclinic connection vanishes, leaving the attracting closed curve Γ_a, to which the unstable branch W_2^U tends. The focus cycle is still attracting, but reached only by the unstable branch W_1^U. The two stable branches of the saddle separate the basins of attraction of the focus cycle and the attracting curve, and have the repelling curve Γ_u as common limit set.

Bifurcations similar to those described in Figs. 7 and 10 are known to occur for flows in some resonant cases of the supercritical Neimark–Hopf bifurcation (see [13]), and also in maps (see e.g., [14]). Recently, in [1] similar bifurcations have been observed in families of maps which have a fixed point loosing stability both via a supercritical N–H bifurcation and a supercritical pitchfork (or flip) bifurcation. In this latter paper, the analysis has been performed along a bifurcation path belonging to the instability region and connecting the two bifurcation curves, and it is also shown that homoclinic connections are substituted by homoclinic tangles (with chaotic dynamics), which is the situation most frequently observed in maps. In our model, we have not detected such kind of phenomena, even if the numerical investigations have been performed using up to nine decimal numbers to approximate the bifurcation values. Obviously, this does not exclude the existence of homoclinic tangles; it simply proves that, if they occur, they involve a very narrow range of the parameters.

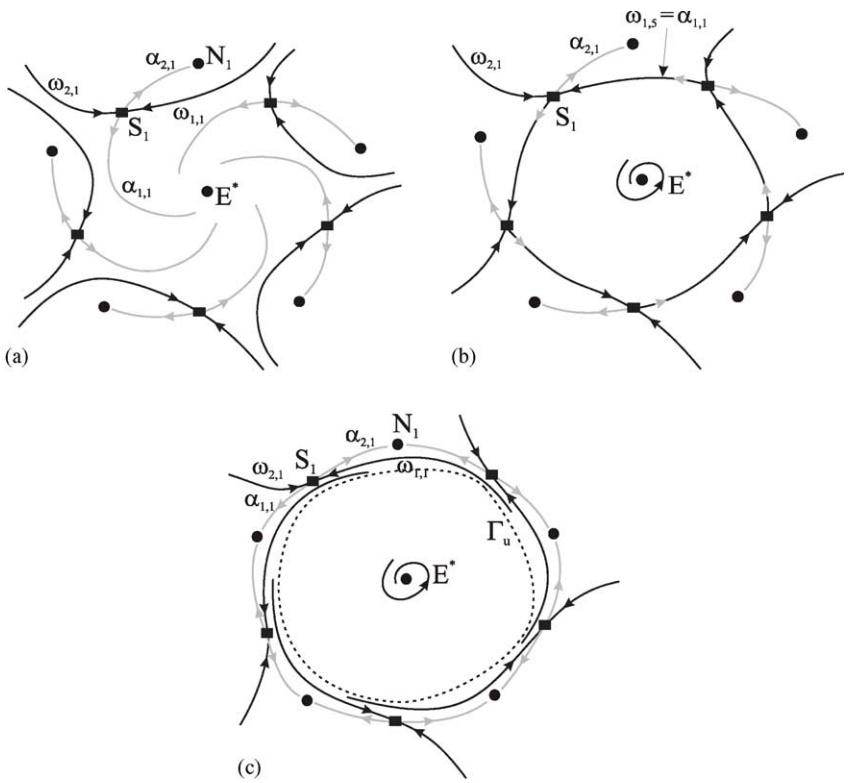

Fig. 11. Qualitative representation of an homoclinic connection which may cause the appearance of a repelling closed invariant curves and a saddle–node connection.

3.3. Generic homoclinic connection and saddle–node connection

In the previous subsections, we have seen, by numerical investigation, how the closed invariant curves Γ_u and Γ_a (existing when the parameters belong to the white strip in Fig. 3, below the N–H bifurcation curve) may appear by global bifurcations involving a saddle cycle (and the example has been taken considering the parameters close to the origin of the $2/9$ periodicity tongue).

Clearly, some global bifurcation must occur in the transition from the gray region to the white strip in Fig. 3, and it is very difficult to investigate (as we cannot be helped from some local approximation of our map). A typical numerical observation is the one already shown in Fig. 1a, when the parameters are in the point A in Fig. 3. That is, we often observe the instantaneous appearance of two closed curves, very close to each other, as in Fig. 1a. Let us formulate a possible mechanism: We conjecture that they appear via a bifurcation similar to the one represented in Fig. 7, involving cycles of very high period and an attracting node (instead of a focus). Due to the high period, the attracting saddle–node connection seems to have quasiperiodic trajectories, and the node explains why the repelling and the attracting invariant curves are so close to each other (the manifolds are not spiraling around a focus).

Our conjecture is summarized in the qualitative sketch of the homoclinic connection given in Fig. 11 (involving a node cycle of period 5).

To conclude this section, we remark that the periodicity tongue considered in this section is not the unique one. For example, a 3/13 periodicity tongue has been observed and close to its origin an attracting period 13 focus-cycle exists (for example, at $\lambda = 0.882321$ and $k = 6.903406$). Another example is a 3/14 periodicity tongue, and close to its origin an attracting period 14 focus-cycle exists (for example, at $\lambda = 0.7875$ and $k = 7.938515$). That is, also in these periodicity tongues we have observed the same mechanisms of bifurcation as those described for the $2/9$ periodicity tongue.

4. Conclusion

In a discrete dynamical system, i.e., an iterated map, the global bifurcations involving closed invariant curves have been less investigated, and several open problem are still present, as remarked in [13]. In particular, the saddle–node bifurcations of closed invariant curves (given by the merging of two closed invariant curves, one attracting and one repelling, followed by their appearance/disappearance), quite common in continuous flows, are instead exceptions when we deal with two-dimensional maps.

This paper focus on the open problem related to the mechanism giving rise to the appearance/disappearance of two invariant closed curves, one attracting and one repelling, in two-dimensional maps.

Considering a duopoly model in which the Cournot equilibrium point coexists with an attracting closed curve and it is destabilized through a subcritical N–H bifurcation, we have shown that such a mechanism may be associated with a saddle-connection. This saddle-connection, also called *homoclinic connection*, is defined as a closed invariant curve formed by the merging of a branch of the stable set of a periodic point of a saddle cycle with the unstable branch of another periodic point of the same saddle, thus forming a closed connection among the periodic points of the saddle. It is a structurally unstable situation, which causes a bifurcation between two qualitatively different dynamic behaviors. As this kind of bifurcation cannot be predicted by a local investigation, it can be classified as a *global bifurcation*.

In the model, here considered, homoclinic connections causing the appearance disappearance of closed invariant curves are associated to a subcritical N–H bifurcation and occur when the fixed point is still stable. Approaching the N–H bifurcation the unstable invariant closed curve becomes smaller and smaller and merges with the fixed point at the bifurcation, leaving the stable invariant closed curve as unique attractor. In discrete models, this sequence of bifurcations, also called *crater bifurcation* in the economic literature (see [12]), seems to be a typical situation in which to observe the scenario we have described. But this scenario may arise in different situations, not necessarily involving a subcritical N–H bifurcation. For example, it has been observed also in [1], along a bifurcation path which connects a pitchfork bifurcation curve to a supercritical Neimark–Hopf one.

Given the attention paid in the economic literature to the onset of endogenous, long-run fluctuations in economic systems, the bifurcation scenario we have detected may find important applications. Indeed, it implies multistability situations and may deserve to explain phenomena like hysteresis loops and catastrophic transitions.

Acknowledgments

The authors thank the referee for his many valuable suggestions and remarks. The usual disclaimer applies. This work has been performed under the activities of the national research project “Nonlinear Models in Economics and Finance: Complex Dynamics, Disequilibrium, Strategic Interaction” , MIUR, Italy.

References

[1] A. Agliari, G.I. Bischi, R. Dieci, L. Gardini, Global bifurcations of closed invariant curves in two-dimensional maps: A computer assisted study, International Journal of Bifurcation and Chaos 15 (2005), in press.
[2] A. Agliari, L. Gardini, T. Puu, The dynamic of a triopoly dynamic game, Chaos, Solitons and Fractals 11 (2000) 2531–2560.
[3] A. Agliari, L. Gardini, T. Puu, Global bifurcation in duopoly when the fixed point is destabilized via a subcritical Neimark bifurcation, International Game Theory Review, in press.
[4] A. Agliari, T. Puu, A Cournot duopoly with bounded inverse demand function, in: T. Puu, I. Sushko (Eds.), Oligopoly and Complex Dynamics: Tools and Models, Springer-Verlag, New York, 2002, pp. 171–194.
[5] J. Bertrand, Théorie mathématique de la richesse sociale, Journale des Savants 48 (1883) 499–508.
[6] G.I. Bischi, M. Kopel, Equilibrium selection in a nonlinear duopoly game with adaptive expectations, Journal of Economic Behavior and Organization 46/1 (2001) 73–100.
[7] G.I. Bischi, M. Kopel, Long run evolution, path dependence and global properties of dynamic games: a tutorial, Cubo A Mathematical Journal 5 (2003) 437–468.
[8] E.H. Chamberlin, The Theory of Monopolistic Competition, Harvard University Press, Cambridge, MA, 1932.
[9] A. Cournot, Recherches sur les principes mathématiques de la théorie des richesses, Hachette, Paris, 1838.
[10] F.Y. Edgeworth, La teoria pura del monopolio, Giornale degli Economisti 15 (1897) 13–31.
[11] J. Guckenheimer, P. Holmes, Nonlinear Oscillations. Dynamical Systems and Bifurcations of Vector Fields, Springer-Verlag, New York, 1997.
[12] C. Kind, Remarks on the economic interpretation of Hopf bifurcation, Economic Letters 62 (1999) 147–154.
[13] H.W. Kuznetsov, Elements of Applied Bifurcation Theory, second ed., Springer-Verlag, New York, 1998.
[14] C. Mira, Chaotic Dynamics. From the One-dimensional Endomorphism to the Two-dimensional Noninvertible Maps, World Scientific, Singapore, 1987.

[15] A. Norin, T. Puu, Cournot duopoly when the competitors operate under capacity constraints, Chaos, Solitons and Fractals 18 (2003) 577–592.
[16] T. Puu, Chaos in duopoly pricing, Chaos, Solitons and Fractals 1 (1991) 573–581.
[17] T. Puu, Attractors, Bifurcations & Chaos. Nonlinear Phenomena in Economics, Springer-Verlag, New York, 2003.
[18] T. Puu, I. Suskho (Eds.), Oligopoly and Complex Dynamics: Tools and Models, Springer-Verlag, New York, 2002.
[19] T. Poston, I. Stewart, Catastrophe Theory and its Applications, Pitman Ltd., London, 1978.
[20] D. Rand, Exotic phenomena in games and duopoly models, Journal of Mathematical Economics 5 (1978) 173–184.
[21] J.B. Rosser, From Catastrophe to Chaos: A General Theory of Economic Discontinuities, Kluwer Academic, Boston, 2000.
[22] J.M.T. Thompson, H.B. Stewart, Nonlinear Dynamics and Chaos, Whiley, New York, 1986.
[23] E. Ott, Chaos in Dynamical Systems, Cambridge University Press, Cambridge, 1993.
[24] Z.T. Zhusubaliyev, E. Mosekilde, Bifurcations and Chaos in Piecewise-smooth Dynamical Systems, World Scientific, Singapore, 2003.